Contrast-Enhanced Ultrasonography for Real-Time Monitoring of Interstitial Laser Thermal Therapy in the Focal Treatment of Prostate Cancer

Mostafa Atri
University Health Network

Mark R. Gertner
Ryerson University

Masoom A. Haider
University Health Network

Robert A. Weersink
Ryerson University

John Trachtenberg
University of Toronto

Please Cite:
Atri, M., Gertner, M. R., Haider, M. A., Weersink, R. A., & Trachtenberg, J. (2009). Contrast-enhanced ultrasonography for real-time monitoring of interstitial laser thermal therapy in the focal treatment of prostate cancer. *Canadian Urological Association Journal, 3*(2), 125–130.
doi:10.5489/cuaj.1044

Contrast-enhanced ultrasonography for real-time monitoring of interstitial laser thermal therapy in the focal treatment of prostate cancer

Mostafa Atri, MD;[*] Mark R. Gertner;[†‡] Masoom A. Haider, MD;[*] Robert A. Weersink;[†‡] John Trachtenberg, MD[§]

Abstract

Introduction: We report a case study of the application of contrast-enhanced ultrasonography (CEUS) for intraoperative monitoring of thermal ablation of a single focus of prostate cancer.

Methods: A patient presented with biopsy-proven, solitary-focus, low-risk prostate cancer and was recruited into a clinical trial of interstitial laser thermal focal therapy. Multiparametric magnetic resonance imaging (MRI) was used to locate the single dominant focus, and photothermal ablation was performed at the tumour site under the guidance of transrectal ultrasonography. Transrectal CEUS using systemic bolus injections of the intravascular contrast agent Definity was performed immediately before, several times during and on completion of therapy. Lesions observed on CEUS were compared with treatment effect as measured by tissue devascularization on 1-week gadolinium (Gd)–enhanced MRI.

Results: Baseline images showed CEUS contrast-agent signal throughout the prostate. During and after treatment, large hypocontrast regions were observed surrounding the treatment fibres, indicating the presence of an avascular lesion resulting from photothermal therapy. Lesion size was found to increase during the delivery of thermal energy. Lesion size measured using CEUS (16 × 11 mm) was similar to the 7-day lesion measured using Gd-enhanced T_1-weighted MRI.

Conclusion: Focal therapy for prostate cancer requires both complete treatment of the dominant tumour focus and minimal morbidity. The application of CEUS during therapy appears to provide an excellent measure of the actual treatment effect. Hence, it can be used to ensure that the therapy encompasses the whole target but does not extend to surrounding critical structures. Future clinical studies are planned with comparisons of intraoperative CEUS to Gd-enhanced MRI at 7 days and whole-mount pathology samples.

Can Urol Assoc J 2009;3(2):125-30

Résumé

Introduction : Nous décrivons un cas d'application de la technique d'échographie de contraste pour la surveillance peropératoire pendant l'ablation thermique d'un cancer de la prostate à foyer unique.

Méthodologie : Le patient présentait un cancer de la prostate à faible risque et à foyer unique confirmé par biopsie et a été inscrit à un essai clinique portant sur la thérapie thermique interstitielle par laser. Après une épreuve d'IRM à paramètres multiples en vue de localiser le foyer dominant unique, on a procédé à une ablation photothermique guidée par échographie transrectale. On a effectué une échographie transrectale à l'aide d'injections bolus intravasculaires de l'agent de contraste Definity immédiatement avant l'ablation, de même que plusieurs fois pendant l'intervention et à la fin de celle-ci. Les lésions observées lors de l'échographie de contraste ont été comparées à l'effet du traitement, tel que mesuré par la dévascularisation tissulaire lors d'une épreuve d'IRM avec injection de Gd une semaine plus tard.

Résultats : Les images initiales montrent le signal de l'agent de contraste dans toute la prostate. Pendant et après le traitement, de grandes zones d'hypocontraste ont été observées autour des zones de traitement, indiquant la présence d'une lésion avasculaire causée par la thérapie photothermique. La taille de la lésion s'est accrue pendant la libération de l'énergie thermique. La taille de la lésion, telle que mesurée par échographie de contraste (16 × 11 mm) n'avait pas changé une semaine plus tard lors de l'épreuve d'IRM T_1 avec injection de Gd.

Conclusion : La thérapie focale appliquée à la prostate requiert le traitement complet du foyer tumoral dominant et une morbidité minimale. Le recours à l'échographie de contraste durant le traitement semble un excellent moyen de mesurer l'effet réel du traitement. On peut donc l'utiliser pour assurer que le traitement englobe toute la zone cible sans s'étendre aux structures adjacentes. D'autres études cliniques comparant les résultats à ceux de l'IRM avec injection de Gd après 7 jours et des échantillons anatomopathologiques *in toto* sont prévues.

Introduction

Prostate cancer is widely believed to be the most common cancer in men and the third most common cause of cancer-related death in men.[1] Many patients now present with low-grade and low-volume disease that offers minimal risk of morbidity or mortality. Focal ablative therapy,

a new paradigm of treatment designed for selective therapeutic destruction of only the region of malignant tumour tissue within the prostate, may be a viable treatment alternative for these patients.[2,3] A histological analysis of over 900 prostatectomy specimens removed for prostate cancer suggests that a solitary dominant lesion is the source of extracapsular disease in over 80% of patients and is thus the likely source of extracapsular spread.[4] Destruction of this single site is therefore likely to significantly decrease the risk of progression and increase cancer control with minimal side effects. Focal ablative therapy offers the ability to preserve the healthy areas of the prostate while posing less risk of damage to intra- and periprostatic critical structures, therefore reducing perioperative morbidity compared with the standards of care (i.e., radical prostatectomy or radiotherapy) and does not preclude further therapy should it be required.

Critical to the success of focal ablative therapy is the ability to monitor the intended ablative damage in real time to ensure that the entire tumour target is destroyed while unaffected prostate and periprostatic critical structures are spared. This is most easily done with diagnostic imaging. Contrast-enhanced ultrasonography (CEUS) using intravascular microbubble agents has been developed to aid in diagnosing disease by defining regions of abnormal blood perfusion or vascular filling patterns, and as a method for local delivery of drugs.[5] CEUS has also been used to assess treatment response for ablative therapies such as radiofrequency ablation[6–9] and high-intensity focused ultrasonography,[10] typically several days after the therapy. Tissue changes following radiofrequency ablation of canine prostates[6] have been monitored 10–15 minutes after completion of therapy. In these applications, the avascular volume created by the ablative therapy manifests as an area of absence of ultrasonography signal on CEUS.

Blood flow monitoring during focal ablative therapy with real-time CEUS is potentially beneficial because it allows the implementation of a longer treatment period and/or adjustments to planned energy or power delivery schemes for regions of the prostate associated with incomplete loss of blood flow signal, which is likely an indicator of incomplete tumour ablation. To date in the many preclinical and few clinical applications of focal ablative therapy, magnetic resonance imaging (MRI) or computed tomography with or without contrast agents have been used to assess treatment completeness.[11,12] These approaches take place days to weeks after the initial procedure, creating the need for a repeat visit for those patients who may be offered further ablation. This can potentially be prevented with optimum ablation at the time of the initial procedure. We report on the use of CEUS to monitor the progression of focal interstitial laser thermal therapy for prostate cancer, in real time. This approach provides the opportunity to adjust treatment delivery to ensure coverage of the planned target volume while minimizing treatment-related morbidity to vital surrounding structures.

Methods

Interstitial laser thermal therapy with monitoring of treatment response using real-time transrectal CEUS was performed on our patient as part of a 12-patient clinical trial testing the safety of using MRI-targeted, ultrasonography-guided interstitial laser thermal therapy for the focal treatment of prostate tumours. The treatment protocol, including the use of microbubble CEUS, was approved by the institutional review board of the hospital.

The patient presented with biopsy-proven, solitary-focus, low-risk prostate cancer (Gleason grade 6, 1 core of 11 positive, with 5% tumour volume in this biopsy) and received multiparametric (T_2- and diffusion-weighted) MRI to locate the tumour. Apparent diffusion coefficient maps were generated from the diffusion-weighted images and interpreted as described previously.[13] Image sets from MRI were imported into the brachytherapy-planning software program VariSeed (Varian, Inc.) and the prostate and tumour were manually traced.

The interstitial laser thermal therapy procedure was performed under general anesthetic, with the patient discharged home the same day. The patient was placed in the lithotomy position. Using a brachytherapy stabilizing apparatus with modified template grid (model RTP6000, North American Scientific, Inc.) and an ultrasonography system (Pro Focus console with model 8848 transrectal probe, BK Medical), the suspicious region identified by MRI was registered to the ultrasounds using VariSeed to enable targeted insertion of the treatment probes to this site. The registration in Variseed is limited to a rigid body registration. Therefore, to account for variations in the shape of the prostate

between MRI and ultrasonography, the planned target volume increased to 4 times the volume of the traced tumour. Photothermal therapy was performed with 2 Indigo Optima Lasers (Ethicon, Inc.), each with a single source fibre delivering light at the wavelength 830 nm.[14,15] Each laser was operated in the adaptive monitoring mode, in which the power of the laser is controlled by feedback of the temperature at the laser probe tip. The initial laser power was set at 15 W for each fibre and the control temperature was set at 100°C. As the temperature measured by the laser fibre probe quickly increased to 100°C, the power delivered by the laser quickly decreased and stabilized at about 2 W. Treatment lasted 12 minutes in total, delivering a total energy of 2.88 kJ. Used separately, each laser fibre typically creates ellipsoid volumes of coagulation 1.5 cm in length with a maximum diameter of 1.0 cm, and was therefore sufficient to encompass the patient's tumour volume (0.25 cm^3). Three fluoro-optic thermometer probes (Luxtron Corp.) were placed in the prostate; 1 at the expected ablation boundary to ensure complete treatment of the target volume and 1 each near the rectum and urethra to ensure temperatures in these critical regions remained at safe levels.

CEUS was performed using several intravenous bolus injections of 0.2 mL Definity followed by a 10-mL saline flush. Continuous low mechanical index CEUS was performed after insertion of all probes but before laser therapy, at the 5-minute time point during heating, immediately after heating, and 5 minutes after the end of heating, using the same BK Medical ultrasonography system that was used for needle guidance but with the system set to contrast imaging mode with pulse inversion.

The volume of ablated prostate tissue was measured on pelvic T_2- and gadolinium (Gd)–enhanced T_1-weighted MRI performed 1 week after treatment using methods previously described for focal ablation.[16] Magnetic resonance imaging scans were imported and registered to similar anatomical features in Variseed. The edge of the prostate was traced on the T_2-weighted series and intraprostatic devascularized areas were identified by tracing dark areas on the Gd-enhanced T_1-weighted series.

Results

Based on the preoperative T_2-weighted MRI and apparent diffusion coefficient MRI, the patient's tumour was found to be located in the midposterior region of the prostate, with a volume of 0.25 cm^3. Location of tumour in this region was also confirmed with 12-core biopsy. There were no other foci of tumour detected in the prostate. Full treatment of the tumour target required the insertion of 2 treatment fibres, separated by 10 mm and positioned within the same axial plane.

Figure 1 (A) shows an axial ultrasound of the midsection of the prostate after treatment fibres and temperature sensors were inserted. Figure 1 (B–E) shows contrast-enhanced ultrasounds each acquired about 30 seconds after systemic injection of a bolus of Definity. Images were acquired immediately before laser thermal therapy (Fig. 1B), 5 minutes after the start of therapy (Fig. 1C), after the completion of the 12 minutes of therapy (Fig. 1C) and 5 minutes after the completion of the laser thermal therapy (Fig. 1E). Before treatment, contrast agent was observed throughout the prostate, with some shadowing of the ultrasonography signal caused by the fibres and catheters evident posteriorly. After treatment started, a large avascular zone surrounded the 2 treatment fibres, about 14 mm in maximum axial diameter, increasing to about 16 mm at the end of treatment (length not shown). The short anteroposterior axis of the lesion was about 11 mm in diameter, but difficult to determine accurately because of the anterior shadowing of the signal. The microbubble contrast agent acts essentially as an intravascular blood perfusion contrast, and so the signal void indicates the presence of a growing avascular region during treatment.

Figure 2 compares the axial CEUS image acquired 5 minutes after the laser therapy to Gd-enhanced (Fig. 2B) and T_2-weighted (Fig. 2C) MRI acquired 7 days after the procedure. Contours of the prostate and lesion are shown on each image. The avascular volume was measured to be 1.2 cm^3 based on the Gd-enhanced MRI, significantly larger than the planned tumour target. Like the microbubble CEUS, the Gd-enhanced MRI also provides blood perfusion contrast, with the absence of signal indicating avascular tissue. In a previous preclinical study, we found that there was good spatial correlation between photodynamic therapy–induced hemorrhagic necrosis and unenhanced regions on Gd-enhanced T_1-weighted images.[17] Therefore the Gd-enhanced MRI provides a reasonable indicator of the shape and location of the treatment-induced avascular lesion. The size of

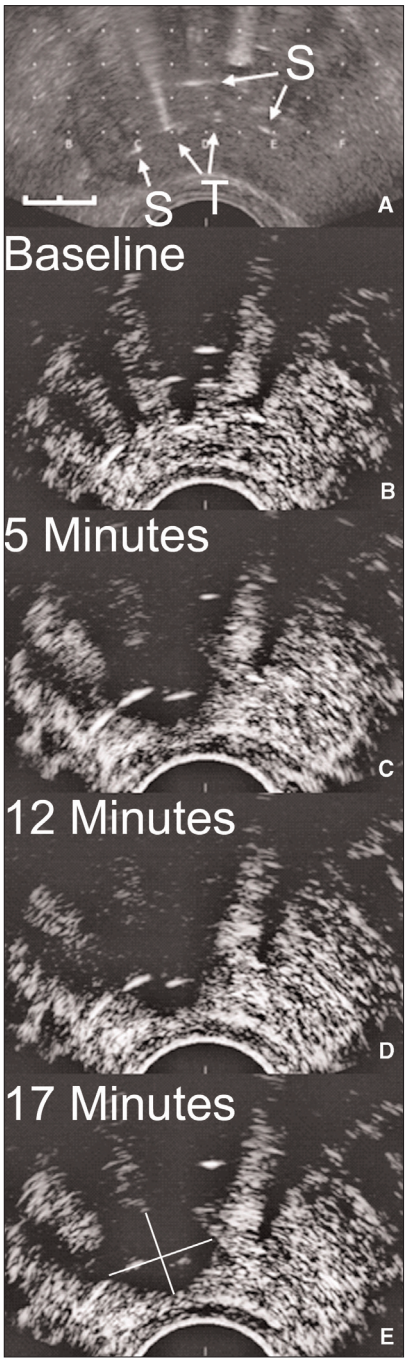

Fig. 1. Axial ultrasounds of the midsection of the prostate after treatment fibres and temperature sensors have been inserted. Standard axial image showing treatment fibres **(T)** and temperature monitoring probes **(S)**. Scale on lower left is 10 mm in length **(A)**. Contrast-enhanced low mechanical index images taken about 1 minute after multiple bolus injections of 0.2 mL of Definity. Images were acquired immediately before laser thermal therapy **(B)**, 5 minutes after the start of therapy **(C)**, after the completion of the 12-minute therapy **(D)** and 5 minutes after the completion of the laser thermal therapy **(E)**.

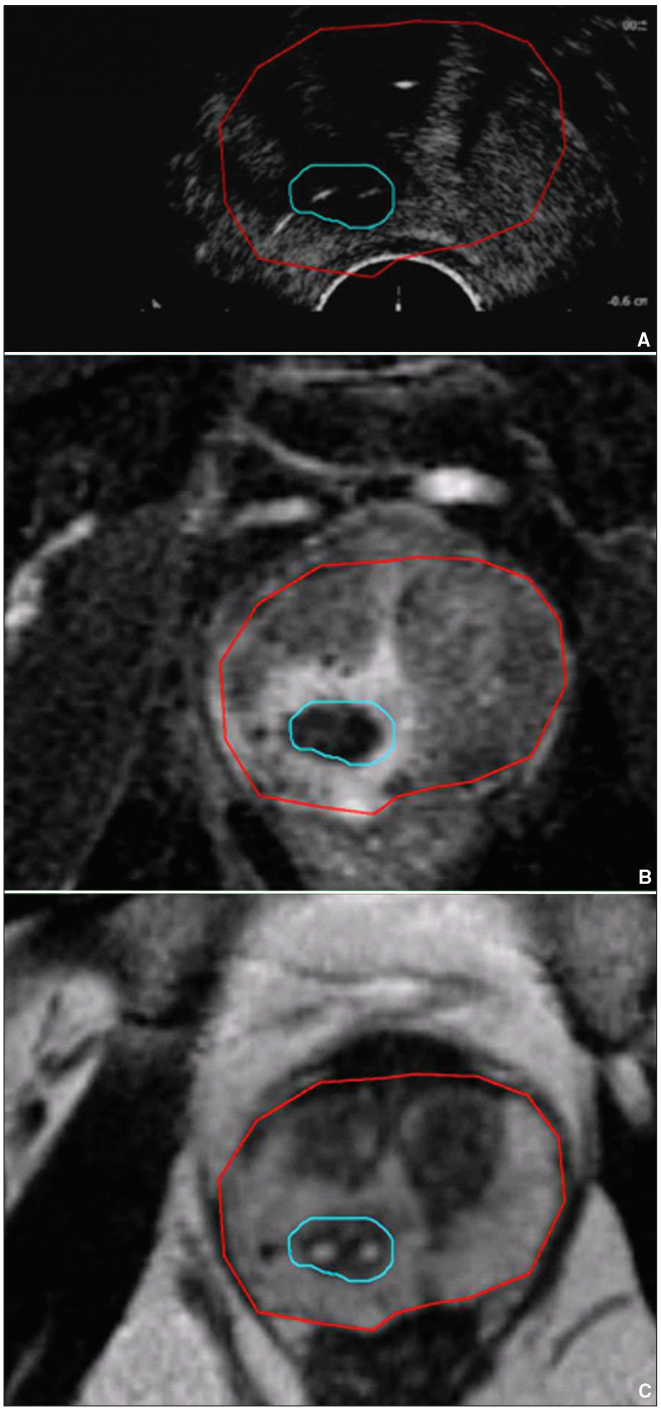

Fig. 2. Comparison of the axial low mechanical index contrast-enhanced ultrasound acquired 5 minutes after the laser therapy **(A)** to Gd-enhanced T_1-weighted magnetic resonance imaging (MRI) scan **(B)** and T_2-weighted MRI scan acquired 7 days after the procedure without an endorectal coil **(C)**. The prostate contour, shown in red, was traced from the T_2-weighted MRI scan, and the treatment effect contour, shown in blue, was traced from the Gd-enhanced T_1-weighted MRI scan. The positions of the fibres are evident as white spots within the T_2-weighted image.

the avascular lesion is essentially identical on both CEUS and Gd-enhanced MRI. A hyperemic zone of about 2 mm surrounds the lesion in the Gd-enhanced MRI scan, indicating inflamed, hyperemic, hemorrhaged and congested tissue, which is a physiological response to tissue heating. This has been previously observed in microwave thermal studies of canine prostates.[18]

Discussion

We have demonstrated what is to our knowledge the first application of microbubble CEUS as a means of monitoring the progress of a thermally coagulative therapy in prostate tissue during treatment. Since the coagulative therapy shuts down blood perfusion, treatment effect is evident by the absence of CEUS signal, with strong contrast between viable tissue and nonviable tissue.

Current active therapies for prostate cancer are associated with significant morbidity. In patients with low-risk disease, focal therapy for identified localized tumours provides a promising alternative with maximal effect and minimal morbidity. The efficacy of a focal therapy, such as interstitial laser thermal therapy, would be improved if there were methods of measuring the treatment response during treatment. Such response monitoring would ensure that the treatment fully encompassed the planned target volume, while sparing vital critical tissue. Tissue temperature can be monitored using MRI thermometry, providing 3-dimensional maps of tissue temperature in real time. However, such monitoring may be cost-prohibitive for most treatment centres. Microbubble CEUS, however, provides a measure of treatment effect in real time using the same imaging platform used in guiding the fibre placement. Consequently, therapy can be adjusted as it progresses to ensure both safety and efficacy. For example, in the case of laser thermal therapy, if the coagulation boundary is nearing the rectum, laser power may be reduced to avoid thermal damage. Furthermore, with real-time CEUS, if it becomes apparent that the planned number of treatment fibres will not cover the planned target volume, the treatment may be suspended briefly while additional source fibres are inserted to cover this region.

For the current clinical trial, treatment effect is measured by 7-day Gd-enhanced MRI, which has been shown to provide excellent correspondence with histological measures of treatment effect.[16,17] Based on the example described here, the coagulated lesion measured by intraoperative CEUS appears to correspond well with the lesion measured using Gd-enhanced MRI at 7 days, suggesting that intraoperative CEUS provides a promising measure of the actual treatment effect. Further detailed studies are planned with more patients to confirm this correspondence, and where possible, to compare treatment effect measured with CEUS to whole-mount pathology samples of patients who subsequently undergo radical prostatectomy.

From the *Department of Medical Imaging, University Health Network and Mount Sinai Hospital, Toronto, Ont., the †Division of Biophysics and Bioimaging, University Health Network, Toronto, Ont., the ‡Department of Physics, Ryerson University, Toronto, Ont., and the §Department of Surgical Oncology, University Health Network and Department of Surgery, University of Toronto, Toronto, Ont.

Acknowledgements: This work was supported by the Muzzo Fund of the Princess Margaret Hospital Foundation and the Guided Therapeutics Program of the University Health Network. Technical support was also provided by BK Medical.

This article has been peer reviewed.

Competing interests: None declared.

References

1. Jemal A, Siegel R, Ward E, et al. Cancer statistics, 2007. *CA Cancer J Clin* 2007;57:43-66.
2. Eggener SE, Scardino PT, Carroll PR, et al. Focal therapy for localized prostate cancer: a critical appraisal of rationale and modalities. *J Urol* 2007;178:2260-7.
3. Bostwick DG, Onik G. Inauguration of the prostate cancer focal therapy debate. *Urology* 2007;70:1-2.
4. Ohori M, Eastham JA, Koh H, et al. Is focal therapy reasonable in patients with early stage prostate cancer (CAP) — an analysis of radical prostatectomy (RP) specimens. *J Urol* 2006;175:507.
5. Ferrara K, Pollard R, Bordeni M. Ultrasound microbubble contrast agents: fundamentals and application to gene and drug delivery. *Annu Rev Biomed Eng* 2007;9:415-47.
6. Liu JB, Merton DA, Wansaicheong G, et al. Contrast enhanced ultrasound for radio frequency ablation of canine prostates: initial results. *J Urol* 2006;176:1654-60.
7. Wen YL, Kudo M, Zheng RQ, et al. Radiofrequency ablation of hepatocellular carcinoma: therapeutic response using contrast-enhanced coded phase-inversion harmonic sonography. *AJR Am J Roentgenol* 2003;181:57-63.
8. Cioni D, Lencioni R, Rossi S, et al. Radiofrequency thermal ablation of hepatocellular carcinoma: using contrast-enhanced harmonic power Doppler sonography to assess treatment outcome. *AJR Am J Roentgenol* 2001;177:783-8.
9. Meloni MF, Goldberg SN, Livraghi T, et al. Hepatocellular carcinoma treated with radiofrequency ablation: comparison of pulse inversion contrast-enhanced harmonic sonography, contrast-enhanced power Doppler sonography, and helical CT. *AJR Am J Roentgenol* 2001;177:375-80.
10. Wondergem N, De La Rosette J. HIFU and cryoablation — non or minimal touch techniques for the treatment of prostate cancer. Is there a role for contrast enhanced ultrasound? *Minim Invasive Ther Allied Technol* 2007;16:22-30.
11. Aron M, Gill IS. Renal tumor ablation. *Curr Opin Urol* 2005;15:298-305.
12. Ahrar K, Wallace MJ, Matin SF. Percutaneous radiofrequency ablation: minimally

invasive therapy for renal tumors. *Expert Rev Anticancer Ther* 2006;6:1735-44.
13. Haider MA, van der Kwast TH, Tanguay J, et al. Combined T2-weighted and diffusion-weighted MRI for localization of prostate cancer. *AJR Am J Roentgenol* 2007;189:323-8.
14. Chandrasekar P, Virdi JS, Kapasi F. Interstitial laser ablation (Indigo) of the prostate; A prospective, randomized study, five year follow-up. *J Urology* 2003;169:392.
15. Daehlin L, Hedlund H. Interstitial laser coagulation in patients with lower urinary tract symptoms from benign prostatic obstruction: treatment under sedoanalgesia with pressure-flow evaluation. *BJU Int* 1999;84:628-36.
16. Haider MA, Davidson SRH, Kale AV, et al. Prostate gland: MR imaging appearance after vascular targeted photodynamic therapy with palladium-bacteriopheophorbide. *Radiology* 2007;244:196-204.
17. Huang Z, Haider MA, Kraft S, et al. Magnetic resonance imaging correlated with the histopathological effect of Pd-bacteriopheophorbide (Tookad) photodynamic therapy on the normal canine prostate gland. *Lasers Surg Med* 2006;38:672-81.
18. Cheng HL, Haider MA, Dill-Macky MJ, et al. MRI and contrast-enhanced ultrasound monitoring of prostate microwave focal thermal therapy: an in-vivo canine study *J Mag Res Imag*. In press.

Correspondence: Dr. Robert Weersink, University Health Network, 610 University Ave., Toronto ON M5G 2M9; weersink@uhnresearch.ca